The parameter space of gene regulatory networks reveals highly designable phenotypes

Chico Q. Camargo[a,b,c,1] **and Ard A. Louis**[d]

[a]College of Engineering, Mathematics and Physical Sciences, University of Exeter, UK; [b]Oxford Internet Institute, University of Oxford, UK; [c]Systems Biology Doctoral Training Centre, University of Oxford, UK; [d]Rudolf Peierls Centre for Theoretical Physics, University of Oxford, UK

This manuscript was compiled on May 23, 2025

Mathematical modelling has transformed our understanding of biology. This is particularly true in the study of cellular metabolism and behaviour: today, the dynamics of the cell can be described by a series of mathematical models, often containing long lists of parameters, and requiring an even greater number of data points to fit every parameter. These large numbers bring with them a burdensome task: identifying a set of N independent parameters that provides a good model fit means locating a single point within a complex N-dimensional landscape. This also raises an evolutionary question: if the model reproduces reality, how did nature find such set of parameters in first place? In this paper, we study this problem using differential equation models for gene regulatory networks, treating the mapping from the parameters of a model to its dynamic behaviour as a genotype-phenotype map. We present two main results: first, that the fraction of genotype space taken by different phenotypes is unevenly distributed, varying over orders of magnitude, with low-complexity phenotypes corresponding to larger numbers of genotypes. Second, that biological metabolic paths are very designable: they correspond to unusually large fractions of genotype space. Our results indicate that gene regulatory networks show properties already seen in other genotype-phenotype maps, and provide explanations for the evolutionary origin and robustness of gene regulatory circuits. They also hold implications for the study and design of synthetic biological circuits and gene regulatory networks.

genotype-phenotype maps | systems biology | evolutionary biology | gene regulatory networks | gene regulatory networks

"Mathematics is biology's next microscope, only better; biology is mathematics' next physics, only better." (1) This statement by J. E. Cohen summarises the mutually beneficial relationship between mathematical and computational tools and the biological sciences. It rings particularly true for the field of systems biology, where mathematical models are present at multiple biological scales, from stochastic simulations of molecular behaviour (2) to Michaelis-Menten-based differential equations expressing the dynamics of the concentrations of every molecule in a system (3–5), to Boolean dynamics of gene regulatory networks pioneered by Stuart Kauffman (6, 7). Of these three classes, differential equation models have perhaps the longest history of success in modelling cellular processes, being used to describe biochemical networks involved in the cell-division cycle (8–10), circadian rhythm (11–13), metabolic regulation (14), calcium oscillations (15), molecular motors (16), genetic oscillators (17), apoptosis (18), as well as many other processes (19). To take one example, the model presented in Chen et al's study of the budding yeast cell-division cycle (10) is composed by a set of 60 differential equations, mapping the relation between 156 biochemical parameters and a set of 54 variables which encode processes ranging from gene expression to mitotic spindle formation.

Models with so many parameters carry with them the problem of fitting those parameters to experimental data: as the size of the parameter space increases exponentially with the number of parameters of a model, the process of finding the right parameters becomes computationally expensive and potentially intractable. For example, even if every one of the 156 parameters of Chen et al's model were to have only one of four possible values – low, medium, high, or zero – this would imply an parameter space of $4^{156} \approx 10^{94}$ possible combinations, an amount clearly too large to be fully enumerated. Yet, Chen et al's model has been very successful in explaining experimental results, having been used to quantitatively predict phenotype viability, sensitivity to biochemical parameters and mutant behaviour (10, 20–22).

Numbers as large as 10^{94} have been described as *hyperastronomical* (23, 24), as they overshadow even the most gigantic numbers in astronomy. Numbers of this magnitude are often seen in combinatorial problems in science and engineering, such as the number of possible connections in the brain (25), Levinthal's paradox in protein folding (26) and the Hoyle-Salisbury paradox (27, 28) of evolutionary search in the space of all proteins. Hyperastronomical numbers also appear at the core of evolutionary biology, representing the overwhelming amount of possible genomes that can be made with the same genes (29). The examples listed above prove that that nature is used to navigating hyperastronomical spaces of many sorts. Moreover, this also suggests that if a model of a biological system shares enough details with the system it is modelling, the

Significance Statement

Mathematical models have become a very useful tool in predicting and understanding complex biological behaviour. A common task in modern systems biology consists in building large models and finding the parameters that will reproduce the target behaviour, a task that can become very difficult in large parameter spaces. Here we treat the parameter-to-behaviour map as a genotype-phenotype map, and use this approach to list the possible behaviours of a given gene regulatory network, showing which behaviours it is most likely to produce. This has applications to the understanding and design of biological systems, but also suggests an answer for the question of how evolution found such biological behaviours: they are just more common in parameter space.

A.A.L. and C.Q.C. conceived and designed the study. C.Q.C. implemented the models, carried out the analysis and wrote the first draft. Both authors edited the manuscript and gave final approval for publication.

The authors declare no conflicts of interest.

[1]To whom correspondence should be addressed. E-mail: f.camargo@exeter.ac.uk

model parameter space might mirror the hyperastronomical space it models, and might even be navigated in a similar way.

Part of the explanation for how finding parameter values in large parameter spaces is at all possible draws from the concept of *sloppiness* (30–32). Essentially, sloppiness is the degree to which the fit between model and data depends more on certain combinations of parameters than on others. In practice, it is how particular eigenparameters affect the model fit more strongly than others. This effect is observed when the Hessian matrix of the prediction error with respect to the parameters of the model presents a broad eigenvalue distribution (33, 34). In a sloppy model, a small subset of parameter combinations are *stiff*, meaning that small changes in them has a large impact on the fit, while most parameter combinations are *sloppy*, meaning that large changes in those parameter combinations make little difference to the fit. That said, sloppiness is a local property: it depends on a given set of measurements and on a given point in parameter space. A model might be more or less sloppy at different parts of parameter space, or with a different set of measurements (35).

In this study, we provide an explanation for the fitting problem which does not rely on sloppiness, but that is inspired by the biological examples of hyperastronomical spaces described above. The mapping from parameters to behaviours is treated as a genotype-phenotype map, with sets of biochemical parameters as genotypes, and the time series corresponding to different parameter sets as phenotypes. Since both genotypes and phenotypes as defined here can take continuous values, both inputs and the outputs are coarse-grained to generate a discrete input-output map, an approach inspired by the robustness tests in Chen et al's model of the budding yeast (10) and used in the genotype-phenotype maps literature (36, 37). Our results reveal a large variation in the number of genotypes mapping to different phenotypes, and show the wild-type behaviours found in nature correspond to the most designable phenotypes, which might hold implications for their evolutionary origin and robustness.

Defining the genotype-phenotype map

An ordinary differential equation (ODE) model can be understood as a map from a given number of parameters to a set of curves over a continuous variable (typically time). In the case of gene regulatory networks, these parameters correspond to allosteric constants and affinity rates, whose value is the product of a series of biological processes, as information is translated from DNA to amino acid sequences and eventually to protein function. Considering that the likely ranges for the values of such parameters are often unknown, we define the ranges for parameter values using an approach inspired by the robustness sampling in Chen et al's model of the budding yeast (10), by setting all parameters to their wild-type values, multiplied by a random factor in $\{0.25, 0.50, \ldots, 1.75, 2.00\}$ chosen with uniform probability. In the case of Chen et al's model, this space comprises $8^{156} \approx 10^{141}$ parameter combinations, which can be sampled uniformly as described above. While this choice of discretisation is arbitrary, different choices of parameter range and scaling factor produce the same qualitative results at phenotype level, as verified by Dingle et al. (36).

Once genotypes have been discretised, every genotype or parameter set will result in a unique output of the ODE system. However, since many of those outputs are likely to be similar to each other, they might best be identified as the same biological phenotype. To capture this simililarity, the ODE outputs are coarse-grained using two methods.

The first method used here to coarse-grain the outputs is Fink et al.'s "up-down" method (38, 39), which, consists of taking an output curve $y(t)$ calculated in an interval $t \in [0, T]$, calculating its slope dy/dt at intervals of $t = \delta t, 2\delta t, 3\delta t, \ldots$, and taking the sign of dy/dt in every interval: for $j = 1, \ldots, T/\delta t$, if $dy/dt \geq 0$ (or < 0) at $t = j \cdot \delta t$, the j-th bit of the output string is written as a `1` (or a `0`). The resulting string encodes the oscillations of $y(t)$ in a coarse-grained manner: curves with few oscillations will result in strings with long sequences of `0`s and `1`s, while curves with more oscillations will result in more complex strings.

Since a system of ODEs will produce one time series for every variable in the model, each curve might also result in a different coarse-grained binary string, with the biological output of the biochemical reaction network likely being the most biologically informative variable. While this is not always precisely defined, the most meaningful output molecules will typically be located downstream, often at the bottom of the regulatory cascade, regulated by a large number of parameters in the network. This dependence on many parameters is what them the most relevant and informative description of the network's behaviour. The key molecules that best represent the biological output of every gene regulatory network in this study are listed in Table 1. For each ODE system, the time series corresponding to the concentration of the key molecule is then coarse-grained, such that every genotype produces a binary string – which is then taken as its corresponding phenotype.

	Model system	Key molecule
1	Rat growth-factor signaling (34)	Active form of B-Raf
2	*E. coli* carbon metabolism (40)	2-Phosphoglycerate
3	Budding yeast cell-division cycle (10)	CLB2/SIC1 complex
4	Nicotinic acetylcholine receptor (41)	Biliganded acetylcholine
5	Protein kinase cascade (42)	MAP2K
6	*Xenopus* Wnt signalling pathway (43)	Non-active beta-catenin
7	*Drosophila* circadian rhythm (12)	Nuclear PER-TIM
8	*Arabidopsis* circadian rhythm (13)	X protein in nucleus
9	Rat growth-factor signaling (44)	Ras-GDP complex
10	*Drosophila* circadian rhythm (45)	Cytoplasmic Clk-Cyc
11	Generic circadian rhythm (11)	C Protein
12	*In silico* regulatory network (46)	Gene A

Table 1. List of all the differential equation models for gene regulatory networks used in this work, presented originally in the meta-analysis by Gutenkunst et al. (31). The key molecule indicated for every model is the biologically relevant output used in the first phenotype definition.

The second definition of phenotype used in this study considers the whole gene regulatory network rather than a single molecule. The output of an ODE system with m variables over time discretised into n time steps becomes an mn-tuple of real positive numbers. As such, we define phenotypes as the clusters formed by these mn-dimensional points, and define the number of genotypes corresponding to the same phenotype

as the number of points in each cluster.

The two phenotypes defined here represent two main ways of coarse-graining the time series resulting from the ODE models. For the first definition, phenotypes are defined by the relation between consecutive points in a time series, thus making it easier to identify different oscillation patterns. The second definition takes in consideration the all the time series produced by the model, favouring the distinction of different regimes of the concentration of the biomolecules in each gene regulatory network.

Phenotype complexity

The relationship between the number of genotypes mapping to a phenotype and its corresponding phenotype complexity can be quantified using tools from the field of Algorithmic information Theory (AIT) (47). In AIT, the Kolmogorov complexity $K(x)$ of an object x is formally defined as the length of the shortest program that generates x on a universal Turing machine (UTM). Similarly, the algorithmic probability $P(x)$ is defined as the probability that random inputs to a UTM produce output x. While genotype-phenotype maps are not UTMs and Kolmogorov complexity is formally uncomputable, Dingle et al. (36) have derived a relationship between the probability $P(x)$ and a computable approximation $\tilde{K}(x)$ to the $K(x)$, for a general set of computable input-output maps, which includes genotype-phenotypes as the ones used in this study. In this relationship, the probability $P(x)$ that a map will produce output x given random inputs can be bounded as below:

$$P(x) \leq 2^{-a\tilde{K}(x)-b} \quad [1]$$

In the equation above, the constants a and b that depend on the mapping, but not on the output x. And even though equation 1 is an upper bound, it has been shown that random sampling of inputs is likely to produce outputs close to the bound, for a wide range of input-output maps (48).

Given that one of the input-output maps studied by Dingle et al. consists in the mapping from the parameters of a system of ODEs to its dynamics, it is straightforward to see that equation 1 applies to the gene regulatory networks studied here. As such, the complexity of different metabolic phenotypes can be estimated using the Lempel-Ziv algorithm, as described in the Methods section.

Results

Figure 1 shows the distribution of phenotype frequency $P(x)$, for 12 ODE models in this study, for samples of 5×10^6 genotypes for every model. In the figure, $P(x)$ stands for the number of genotypes mapping to a phenotype, divided by the total number of genotypes in the sample.

The two sets of phenotypes in this study, namely the oscillation phenotype and the cluster phenotype, are shown respectively in Figures 1A and 1B. Although both sets of curves reveal long-tailed distributions of phenotype frequencies, there are stark differences between the two sets of distributions: on the left panel, the total number of phenotypes approaches 10^6 for the oscillation phenotypes, while it stays under 10^3 for the cluster phenotypes on the right panel. Moreover, the shape of the distributions in Fig 1A resemble power law distributions, while in Fig 1B they appear closer to log-normal curves.

These differences, however, only exist due to one common characteristic between both phenotypes: in both cases, the distribution of phenotype frequencies is very skewed, with a few high-frequency phenotypes taking over most of genotype space, and most phenotypes corresponding having a very low frequency, meaning they correspond to few genotypes from the sample. It is important to remember that this result comes from a finite sample of genotype space, which might affect the number of observed phenotypes: any phenotype with frequency under 10^{-6} is likely to not be present in a sample of 5×10^6 genotypes.

The plots shown in panels 1C and 1D show the rank of the wild-type phenotype in relation to all other phenotypes, for both phenotype definitions and all gene regulatory networks in this study. Values of 100% and 98.12%, such as the ones corresponding to the wild-type phenotype for the rat growth-factor signaling network (34), indicate that the frequency of its wild-type phenotype is larger than 100% of the neutral sets corresponding to other oscillation phenotypes, and larger than 98.12% of the neutral sets corresponding to other cluster phenotypes.

As shown in both panels, for all networks in this study, the wild-type phenotype has an unusually large neutral set, often having the largest neutral set in the whole genotype-phenotype map (represented as a 100%), with the lowest value observed being 60%. Taking in consideration the bias in the distribution of phenotype frequencies shown in panels 1A and 1B, these results indicate that the phenotype frequency wild-type phenotypes is typically orders of magnitude above the frequency of most other phenotypes.

In addition to the skewed distribution of phenotype frequencies discussed above, the genotype-phenotype maps studied here also show a strong bias towards low-complexity phenotypes, a pattern which has been observed for input-output maps of limited complexity (36), as well as for the mapping between parameters and function in neural networks (49) and for several biological systems (37). This is presented in Figure 2, which shows plots of phenotype frequency $P(x)$ versus phenotype complexity $K(x)$, for all oscillation phenotypes.

Figure 2A shows $P(x)$ versus $K(x)$ for the rat growth-factor signaling network in ref. (44). The purple hull around the majority of the dots in the scatter plot is a visual aid to help in the interpretation of Figure 2B, which shows the hulls corresponding to the frequency-complexity scatter plot for all 12 systems, in the same order as presented in Table 1 and Figure 1C. The plot shown in panel 2A is included as the last plot on the bottom right corner.

Unlike the frequency-rank plots shown in Figure 1 for both phenotype definitions, the frequency-complexity analysis shown in Figure 2 can only be done for the oscillation phenotype. This is because there is no unambiguous way to measure the complexity of a cluster of trajectories in N-dimensional space, as it is not clear how exactly such a measure of "cluster complexity" would capture phenotypic complexity. By contrast, the complexity of an oscillation phenotype as defined here can be easily interpreted: phenotypes showing simple behaviour with regular and periodic oscillations result in lower $K(x)$, whilst phenotypes showing complex behaviour with irregular aperiodic oscillations will yield higher values of $K(x)$. Furthermore, oscillation phenotypes are encoded by binary strings, whose complexity can be easily estimated, as

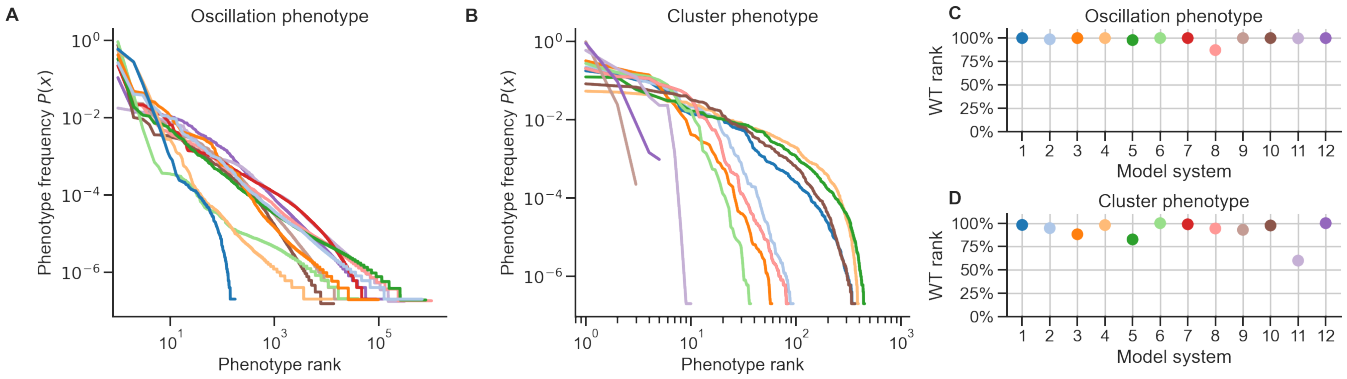

Fig. 1. The distributions of phenotype frequencies are strongly biased. Panels **(A)** and **(B)** respectively show the distribution of phenotype frequencies for the oscillation phenotypes and for the cluster phenotypes, for all 12 gene regulatory networks. Both panels show very uneven distributions of phenotype frequencies, with a few phenotypes taking over most of the 5×10^6 sampled genotypes, and most phenotypes corresponding to only a few genotypes. Panels **(C)** and **(D)** show the rank of the wild-type phenotype in relation to all other phenotypes, for both phenotype definitions and all networks in this study. A value of 98%, for example, indicates that the wild-type's neutral set is larger than 98% of the neutral sets corresponding to other phenotypes for that network.

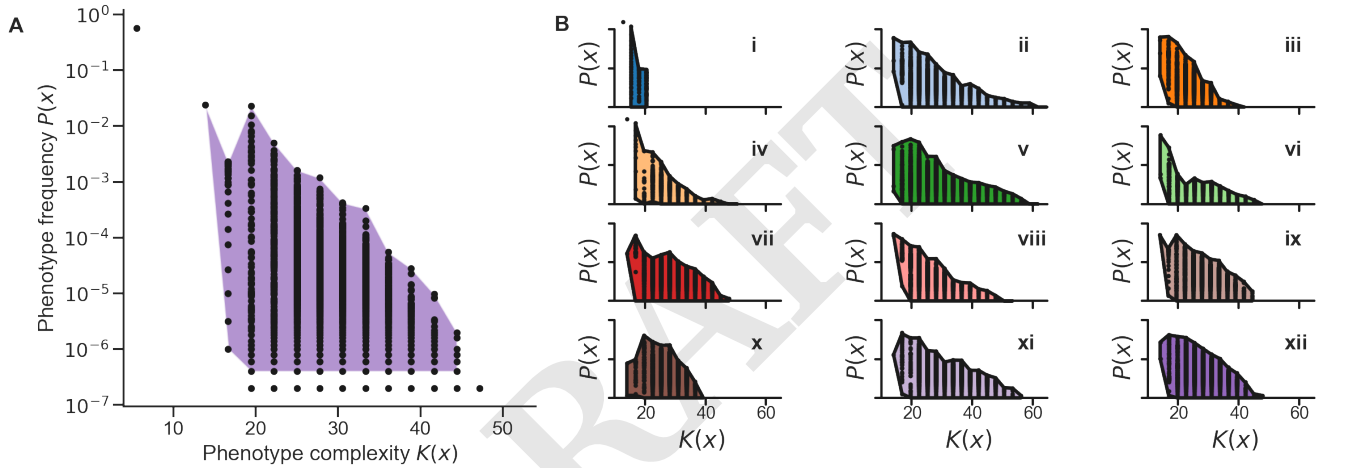

Fig. 2. Genotype-phenotype maps for gene regulatory networks are biased towards simple phenotypes. Panel **(A)** shows a scatter plot of the phenotype frequency versus phenotype complexity for the rat growth-factor signaling network in ref. (44). The purple hull around the majority of the dots in the scatter plot is a visual aid to help in the interpretation of **(B)**, which shows the hulls corresponding to the $P(x)$-$K(x)$ scatter plot for all 12 systems. The plot shown in **(A)** is included as plot xii in panel **(B)**. For all gene regulatory networks, the oscillation phenotype GP map shows shows a strong bias towards low-$K(x)$ phenotypes.

discussed in the Methods section.

Together, the frequency-complexity plots in Figure 2B show a clear pattern: for all gene regulatory networks observed, the oscillation phenotype GP map shows shows a strong bias towards low-$K(x)$ phenotypes. This is evidenced by the roughly triangular outline of all plots, which indicates that phenotypes with higher frequency typically have lower complexity. This behaviour has been described by Dingle et al. as *simplicity bias* (36).

Discussion

In this paper, we have shown that the genotype-phenotype (GP) map from the biochemical parameters of a gene regulatory network to its dynamics is biased towards producing low-complexity behaviour. We studied this GP map by examining twelve mathematical models of gene regulatory networks across a range of biological systems, from gene regulatory networks in the budding yeast to signalling networks in mammals, and observed that the biases shown by this GP map do not depend on any specific definition of phenotype. Moreover, we found that the largest fractions of genotype space often correspond to the phenotypes presented by wild-type organisms.

The bias towards low-complexity behaviour observed here is not unique to gene regulatory networks, or to differential equation models. This phenomenon, which Dingle et al. call simplicity bias (36), is found in numerous input-output maps, including but not limited to RNA sequence-to-structure maps (36, 50), Boolean gene regulatory networks (51), stochastic models in financial mathematics (36) and parameter-to-function maps in deep neural networks (49). This pattern has also been reported for genotype-phenotype maps for protein quaternary structures and macromolecular self-assembly (37).

The relevance of simplicity bias is particularly clear in the context of evolutionary biology. The search spaces explored by evolution have long been said to be of hyperastronomical size, meaning that the number of possible combinations of different alleles easily surpass astronomical numbers such as the number of stars in a galaxy, or even the number of subparticles in the visible universe (24, 29). In practice, this makes it impossible for evolution to fully exhaust a genotype space searching for

one particular DNA or amino acid sequence that might yield a phenotype with desirable properties. However, when that genotype space is part of a GP map where multiple genotypes produce the same few phenotypes, those phenotypes corresponding to larger fractions of genotype space are more likely to be discovered, ultimately making evolutionary dynamics possible. This rationale has been explored at length in the GP map literature (24, 37, 50, 52–54).

Our results suggest that the biased structure of this GP map might have constrained the phenotypic variation of gene regulatory networks available to natural selection, resulting in the very designable phenotypes we observe here. Moreover, due to the simplicity bias in this GP map, the range of phenotypes available to natural selection would be constrained to a set mostly made of simple phenotypes.

Despite the relevance of these results to evolutionary dynamics, it is important to note that gene regulatory networks do not evolve simply by varying the strength of interactions represented by the biochemical parameters studied here. Rather, those networks typically evolve by mutations which result in the addition or subtractions of interactions between biomolecules, thus effectively changing the topology of the network. There is evidence that GP maps of regulatory networks of varying topology also show simplicity bias (51), and a more complete study of the evolution of gene regulatory networks should take both topology and biochemical parameters into account.

The dynamic behaviour of a gene regulatory network makes the task of defining phenotypes more ambiguous than for some of the GP maps such studied by ref. (37), where phenotypes are clearly defined RNA or protein structures. However, given that both phenotype definitions studied in this paper result in GP maps with the same properties as observed Camargo et al's GP maps for gene regulatory networks (51), and considering that those properties are in agreement with the broader GP maps literature, we believe the results reported here do not depend on the biological specifics of any given gene regulatory network, or on any specific implementation of this GP map, and are in fact a common feature of the mapping from a gene regulatory network to its dynamics. Effectively, our results corroborate and expand the results of ref. (37) regarding the ubiquity of simplicity bias in GP maps.

In addition to their implications for evolutionary biology, the results of this study shed light on what makes parameter fitting at all possible, particularly for models with hundreds of parameters, as some of the models presented here. Given that fitting a model does not require finding a specific parameter set, but rather finding *any* parameter set that produces the behaviour observed experimentally, when the target behaviour is highly designable, i.e. when it can be produced by multiple parameter combinations, the task of finding a suitable parameter set goes from seemingly impossible to perfectly feasible. This finding echoes analogous results concerning Levinthal's paradox in protein folding and the Hoyle-Salisbury paradox of evolutionary search: searching for an input is hard, searching for an output is easy (24, 37).

Not only do wild-type phenotypes occupy large volumes in genotype space, but they are also known to be sloppy (31), meaning that some directions in parameter space are more likely to produce phenotype change than others (30–32). Our findings complement the literature on sloppiness, as they indicate that these sloppy wild-type parameter sets have unusually large volumes when compared to other phenotypes for the same gene regulatory network. And unlike the results concerning sloppiness, the findings we present here are global: they are not restricted to specific regions in parameter space, and are not contingent on a set of experimental measurements, which are required for sloppiness estimations (30, 55).

Finally, our results indicate interesting avenues for systems and synthetic biology. If the GP maps of gene regulatory networks show a high degree of redundancy and a strong bias towards simple behaviours, estimating the parameters of a complex metabolic model might not require the usual large and complex arrays of experiments: rather, sampling parameter space and looking for the most designable phenotypes might be a cheaper and faster alternative, drawingg from the redundancies built into the network. Naturally, that also raises important questions about the limit of this sampling method: would this apply to any kind of gene regulatory networks, provided that they show enough variation in the designability and complexity of their phenotypes? How much variation is enough variation? Further work will be necessary to determine the limits of this approach.

Finally, beyong gene regulatory networks, this study shows a powerful example of how simplicity bias and algorithmic information theory might be powerful tools in understanding high-dimensional dynamical systems. Understanding parameter-to-behaviour maps as computable input-output maps might be the key to developing new search algorithms for parameter spaces where optimisation seems an intractable problem – much like evolution itself.

Materials and Methods

Simulating gene regulatory networks. The mathematical models of gene regulatory networks used in this paper are listed in Table 1 were taken from Gutenkunst et al's study of sloppiness in systems of differential equations (31). The models included here describe biological systems ranging from rat growth-factor signaling (34, 44) to *E. coli* carbon metabolism (40) to circadian rhythm in the *Arabidopsis* plant (13). All models were implemented using a mix of custom Python scripts and the open-source modeling environment SloppyCell, version 1.0 (56, 57), a software environment for simulation and analysis of biomolecular networks.

For each biological system, 5×10^6 genotypes were sampled following Chen et al's approach as described above (10), and discretised output curves into 50 time points. The robustness of our results with respect to these implementation choices is discussed in the SI Appendix. Time series were clustered using the implementation of the BIRCH algorithm present in the Scikit-learn Python machine learning library (58), using the Euclidean distance as the clustering distance metric. The BIRCH algorithm is suited for clusters of different density and size, and is often used for large datasets due to its good performance even with limited memory and computational time complexity of $O(N)$ on the number of data points (59, 60). BIRCH has also been used in the context of genotype-phenotype maps: Raman and Wagner used it to cluster the concentration trajectories of signalling molecules, in a genotype-phenotype study of the *Saccharomyces cerevisae* target-of-rapamycin signalling circuit (61). We also follow Raman and Wagner's approach to confirm that the clustering method is indeed separating phenotypes in disjoint clusters, by comparing the distances between phenotypes in the same cluster to distances between phenotypes in different clusters, for all clusters in each system. All results are shown in the SI Appendix.

Measuring phenotype complexity. For the oscillation phenotype, the curve $y(t)$ corresponding to the time series for the concentration of

the output molecule of every network is discretised, and converted into a binary string using Fink et al.'s up-down method (38, 39). Since the complexity of this procedure does not increase with the number of time points in the curve, the full map from the parameters of the ODE model to the binary output strings of the up-down method can be viewed as a limited complexity map. (36). It is worth pointing out that this coarse-graining procedure does not produce any bias towards low-complexity outputs. This has been explained by Dingle et al (36).

The complexity of a string $x = \{x_1...x_n\}$ is estimated using the Lempel-Ziv method, as defined below:

$$C_{LZ}(x) = \begin{cases} \log_2(n), & x = 0^n \text{ or } 1^n \\ \frac{\log_2(n)}{2}[N_w(x_1...x_n) + N_w(x_n...x_1)] & \text{otherwise} \end{cases} \quad [2]$$

where $n = |x|$ and $N_w(x)$ is the number of patterns in the dictionary created by the 1976 Lempel-Ziv algorithm (62). The reason for distinguishing 0^n and 1^n is to correct for the strings 0^n and 1^n, whose complexity scales as $\log_2(n)$ as one only needs to encode n to produce them. Defined this way, the $\tilde{K}(x) = C_{LZ}(x)$ measure produces the correct behaviour for simple, short strings, but also for complex strings in the $n \to \infty$ limit. Finally, taking the mean between the complexity of the forward and reversed strings allows the measure it to have finer grained complexity values. For a more detailed discussion, we point the reader to Dingle et al. (36).

ACKNOWLEDGMENTS. CQC acknowledges the Clarendon Fund and the Systems Biology CDT at the University of Oxford for supporting this research.

1. Cohen JE (2004) Mathematics is biology's next microscope, only better; biology is mathematics' next physics, only better. *PLoS biology* 2(12):e439.
2. Gillespie DT (1976) A general method for numerically simulating the stochastic time evolution of coupled chemical reactions. *Journal of computational physics* 22(4):403–434.
3. Novák B, Tyson JJ (2008) Design principles of biochemical oscillators. *Nature reviews. Molecular cell biology* 9(12):981.
4. Tyson JJ, Albert R, Goldbeter A, Ruoff P, Sible J (2008) Biological switches and clocks. *Journal of The Royal Society Interface* 5(Suppl_1):S1–S8.
5. Chu D, Zabet NR, Mitavskiy B (2009) Models of transcription factor binding: sensitivity of activation functions to model assumptions. *Journal of Theoretical Biology* 257(3):419–429.
6. Kauffman SA (1993) *The Origins of Order: Self-organization and selection in evolution.* (Oxford University Press, USA).
7. Kauffman SA (1969) Metabolic stability and epigenesis in randomly constructed genetic nets. *Journal of theoretical biology* 22(3):437–467.
8. Tyson JJ (1991) Modeling the cell division cycle: cdc2 and cyclin interactions. *Proceedings of the National Academy of Sciences* 88(16):7328–7332.
9. Zwolak JW, Tyson JJ, Watson LT (2005) Globally optimised parameters for a model of mitotic control in frog egg extracts. *IEE Proceedings-Systems Biology* 152(2):81–92.
10. Chen KC, et al. (2004) Integrative analysis of cell cycle control in budding yeast. *Molecular biology of the cell* 15(8):3841–3862.
11. Vilar J, Kueh H, Barkai N, Leibler S (2002) Mechanisms of noise-resistance in genetic oscillators. *Proceedings of the National Academy of Sciences of the United States of America* 99(9):5988.
12. Leloup JC, Goldbeter A (1999) Chaos and birhythmicity in a model for circadian oscillations of the PER and TIM proteins in Drosophila. *Journal of theoretical biology* 198(3):445–459.
13. Locke JC, et al. (2005) Extension of a genetic network model by iterative experimentation and mathematical analysis. *Molecular systems biology* 1(1).
14. Fell D, Cornish-Bowden A (1997) *Understanding the control of metabolism.* (Portland press London) Vol. 2.
15. Dupont G, Goldbeter A (1997) Modelling oscillations and waves of cytosolic calcium. *Nonlinear Analysis: Theory, Methods & Applications* 30(3):1781–1792.
16. Peskin CS, Odell GM, Oster GF (1993) Cellular motions and thermal fluctuations: the brownian ratchet. *Biophysical journal* 65(1):316–324.
17. Goodwin B (1966) An entrainment model for timed enzyme syntheses in bacteria. *Nature* 209(5022):479–481.
18. Fussenegger M, Bailey JE, Varner J (2000) A mathematical model of caspase function in apoptosis. *Nature biotechnology* 18(7):768–774.
19. Tyson JJ, Chen K, Novak B (2001) Network dynamics and cell physiology. *Nature Reviews Molecular Cell Biology* 2(12):908–916.
20. Lovrics A, et al. (2006) Time scale and dimension analysis of a budding yeast cell cycle model. *BMC bioinformatics* 7(1):494.
21. Hancioglu B, Tyson JJ (2012) A mathematical model of mitotic exit in budding yeast: the role of polo kinase. *PLOS ONE* 7(2):e30810.
22. Kraikivski P, Chen KC, Laomettachit T, Murali T, Tyson JJ (2015) From start to finish: computational analysis of cell cycle control in budding yeast. *Npj Systems Biology And Applications* 1:15016.
23. Kauffman SA (1996) *At Home in the Universe: The search for the laws of self-organization and complexity.* (Oxford University Press).
24. Louis AA (2016) Contingency, convergence and hyper-astronomical numbers in biological evolution. *Studies in History and Philosophy of Science Part C: Studies in History and Philosophy of Biological and Biomedical Sciences* 58:107–116.
25. Edelman GM (1998) Building a picture of the brain. *Daedalus* 127(2):37–69.
26. Levinthal C (1969) How to fold graciously. *Mossbauer spectroscopy in biological systems* 67:22–24.
27. Hoyle F (1981) The universe: past and present reflections. *Engineering and Science* 45(2):8–12.
28. Salisbury FB (1969) Natural selection and the complexity of the gene. *Nature* 224(5217):342.
29. Wright S (1932) The roles of mutation, inbreeding, crossbreeding, and selection in evolution. *Proceedings of the Sixth International Congress of Genetics, Ithaca, New York, 1932* pp. 356–366.
30. Waterfall JJ, et al. (2006) Sloppy-model universality class and the Vandermonde matrix. *Physical review letters* 97(15):150601.
31. Gutenkunst RN, et al. (2007) Universally sloppy parameter sensitivities in systems biology models. *PLoS computational biology* 3(10):e189.
32. Chachra R, Transtrum MK, Sethna JP (2012) Structural susceptibility and separation of time scales in the Van der Pol oscillator. *Physical Review E* 86(2):026712.
33. Brown KS, Sethna JP (2003) Statistical mechanical approaches to models with many poorly known parameters. *Physical Review E* 68(2):021904.
34. Brown KS, et al. (2004) The statistical mechanics of complex signaling networks: nerve growth factor signaling. *Physical biology* 1(3):184.
35. Tönsing C, Timmer J, Kreutz C (2014) Cause and cure of sloppiness in ordinary differential equation models. *Physical Review E* 90(2):023303.
36. Dingle K, Camargo CQ, Louis AA (2018) Input–output maps are strongly biased towards simple outputs. *Nature Communications* 9(1):761.
37. evolution paper here. A (1) Symmetry and simplicity spontaneously emerge from the algorithmic nature of evolution. *Science* 1(1).
38. Willbrand K, Radvanyi F, Nadal JP, Thiery JP, Fink TM (2005) Identifying genes from up–down properties of microarray expression series. *Bioinformatics* 21(20):3859–3864.
39. Fink TM, Willbrand K, Brown FC (2007) 1-d random landscapes and non-random data series. *EPL (Europhysics Letters)* 79(3):38006.
40. Chassagnole C, Noisommit-Rizzi N, Schmid JW, Mauch K, Reuss M (2002) Dynamic modeling of the central carbon metabolism of Escherichia coli. *Biotechnology and bioengineering* 79(1):53–73.
41. Edelstein SJ, Schaad O, Henry E, Bertrand D, Changeux JP (1996) A kinetic mechanism for nicotinic acetylcholine receptors based on multiple allosteric transitions. *Biological cybernetics* 75(5):361–379.
42. Kholodenko BN (2000) Negative feedback and ultrasensitivity can bring about oscillations in the mitogen-activated protein kinase cascades. *The FEBS Journal* 267(6):1583–1588.
43. Lee E, Salic A, Krüger R, Heinrich R, Kirschner MW (2003) The roles of APC and Axin derived from experimental and theoretical analysis of the Wnt pathway. *PLoS biology* 1(1):e10.
44. Sasagawa S, Ozaki Yi, Fujita K, Kuroda S (2005) Prediction and validation of the distinct dynamics of transient and sustained ERK activation. *Nature cell biology* 7(4):365–373.
45. Ueda HR, Hagiwara M, Kitano H (2001) Robust oscillations within the interlocked feedback model of Drosophila circadian rhythm. *Journal of theoretical biology* 210(4):401–406.
46. Zak DE, Gonye GE, Schwaber JS, Doyle FJ (2003) Importance of input perturbations and stochastic gene expression in the reverse engineering of genetic regulatory networks: insights from an identifiability analysis of an *in silico* network. *Genome research* 13(11):2396–2405.
47. Li M, Vitányi PM (2008) *An introduction to Kolmogorov complexity and its applications.* (Springer Publishing Company, Incorporated).
48. Dingle K, Pérez GV, Louis AA (2020) Generic predictions of output probability based on complexities of inputs and outputs. *Scientific reports* 10(1):1–9.
49. Valle-Perez G, Camargo CQ, Louis AA (2019) Deep learning generalizes because the parameter-function map is biased towards simple functions in *International Conference on Learning Representations.*
50. Dingle K, Schaper S, Louis AA (2015) The structure of the genotype–phenotype map strongly constrains the evolution of non-coding RNA. *Interface focus* 5(6):20150053.
51. Camargo CQ, Louis AA (2020) Boolean threshold networks as models of genotype-phenotype maps in *Complex Networks XI.* (Springer), pp. 143–155.
52. Manrubia SC, Cuesta JA (2010) Neutral networks of genotypes: Evolution behind the curtain. *arXiv preprint arXiv:1002.2745.*
53. Wagner A (2014) *Arrival of the Fittest: Solving Evolution's Greatest Puzzle.* (Penguin).
54. Schaper S, Louis AA (2014) The arrival of the frequent: how bias in genotype-phenotype maps can steer populations to local optima. *PLOS ONE* 9(2):e86635.
55. Chis OT, Villaverde AF, Banga JR, Balsa-Canto E (2016) On the relationship between sloppiness and identifiability. *Mathematical biosciences* 282:147–161.
56. Myers CR, Gutenkunst RN, Sethna JP (2007) Python unleashed on systems biology. *Computing in Science & Engineering* 9(3):34–37.
57. Gutenkunst RN, et al. (2007) Sloppycell. *See http://sloppycell.sourceforge.net.*
58. Pedregosa F, et al. (2011) Scikit-learn: Machine learning in Python. *Journal of Machine Learning Research* 12:2825–2830.
59. Rafsanjani MK, Varzaneh ZA, Chukanlo NE (2012) A survey of hierarchical clustering algorithms. *The Journal of Mathematics and Computer Science* 5(3):229–240.
60. Madan S, Dana KJ (2016) Modified balanced iterative reducing and clustering using hierarchies (m-BIRCH) for visual clustering. *Pattern Analysis and Applications* 19(4):1023–1040.
61. Raman K, Wagner A (2011) Evolvability and robustness in a complex signalling circuit. *Molecular BioSystems* 7(4):1081–1092.
62. Lempel A, Ziv J (1976) On the complexity of finite sequences. *IEEE Transactions on Information Theory* 22(1):75–81.